Characterization of auxin transporter PIN6 plasma membrane targeting reveals a function for PIN6 in plant bolting

Journal:	*New Phytologist*
Manuscript ID	NPH-MS-2017-24689
Manuscript Type:	MS - Regular Manuscript
Date Submitted by the Author:	13-Jun-2017
Complete List of Authors:	Ditengou, Franck; Albert-Ludwigs-Universitat Freiburg Fakultat fur Biologie, Molecularpflanzenbiologie Gomes, Dulceneia ; Albert-Ludwigs-Universitat Freiburg Fakultat fur Biologie, Molecularpflanzenbiologie Nziengui, Hugues; Albert-Ludwigs-Universitat Freiburg Fakultat fur Biologie, Molecularpflanzenbiologie Kochersperger, Philip; Albert-Ludwigs-Universitat Freiburg Fakultat fur Biologie, Molecularpflanzenbiologie Lasok, Hanna; Albert-Ludwigs-Universitat Freiburg Fakultat fur Biologie, Molecularpflanzenbiologie Medeiros, Violante; Albert-Ludwigs-Universitat Freiburg Fakultat fur Biologie, Molecularpflanzenbiologie Paponov, Ivan; Albert-Ludwigs-Universitat Freiburg Fakultat fur Biologie, Molecularpflanzenbiologie; Norsk Institutt for Biookonomi, Division for Food Production and Society. Horticulture. Nagy, Szilvia ; Semmelweis University, Department of Medical Chemistry, Molecular Biology and Pathobiochemistry Nádai, Tímea ; Centre for Agricultural Research of the Hungarian Academy of Sciences, Department of Plant Cell Biology Mészáros, Tamás; Semmelweis University, Department of Medical Chemistry, Molecular Biology and Pathobiochemistry Barnabas, Beata; Centre for Agricultural Research of the Hungarian Academy of Sciences, Department of Plant Cell Biology Rapp, Katja; Albert-Ludwigs-Universitat Freiburg Fakultat fur Biologie, Molecularpflanzenbiologie Qi, Linlin; VIB-UGent, Center For Plant systems biology Li, Xugang; Universität Freiburg, Institut für Biologie II und Zentrum für Angewandte Biowissenschaften Becker, Claude; Max-Planck-Institut fur Entwicklungsbiologie, Molecular Biology; Gregor Mendel Institute of Molecular Plant Biology GmbH, Genomics and Epigenomics Li, Chuanyou; Chinese Academy of Sciences, Institute of Genetics & Developmental Biology; Doczi, Robert; Royal Holloway, University of London, School of Biological Sciences; Palme, Klaus; Albert-Ludwigs-Universität, Institut für Biologie II /

	Molecular Plant Physiology
Key Words:	Arabidopsis thaliana, Auxin, inflorescence, Stem, Bolting

Characterization of auxin transporter PIN6 plasma membrane targeting reveals a function for PIN6 in plant bolting

Franck Anicet Ditengou[1¥], Dulceneia Gomes[1], Hugues Nziengui[1], Philip Kochersperger[1], Hanna Lasok[1], Violante Medeiros[1], Ivan A. Paponov[1,3], Szilvia K. Nagy[4], Tímea V. Nádai[2], Tamás Mészáros[4,5], Beáta Barnabás[2], Katja Rapp[1], Linlin Qi[6], Xugang Li[1,7], Claude Becker[1,8], Chuanyou Li[6], Róbert Dóczi[2] and Klaus Palme[1,8,9,10,11¥]

[1]Institute of Biology II, Faculty of Biology, University of Freiburg, Schänzlestrasse 1, D-79104 Freiburg, Germany.

[2]Department of Plant Cell Biology, Centre for Agricultural Research of the Hungarian Academy of Sciences, H-2462 Martonvásár, Brunszvik u. 2, Hungary.

[3]NIBIO, Norwegian Institute for Bioeconomy Research, Postvegen 213, 4353 Klepp Stasjon, Norway.

[4]Department of Medical Chemistry, Molecular Biology and Pathobiochemistry, Semmelweis University, H-1094 Budapest, Tűzoltó u. 37-47, Hungary.[5] Research Group for Technical Analytical Chemistry, Hungarian Academy of Sciences - Budapest University of Technology and Economics, H-1111 Budapest, Szt. Gellért tér 4, Hungary.

[6]State Key Laboratory of Plant Genomics, National Centre for Plant Gene Research (Beijing), Institute of Genetics and Developmental Biology, Chinese Academy of Sciences, Beijing 100101, China.

[7]School of Biological Science and Technology, University of Jinan, 336, West Road of Nan Xinzhuang, Jinan 250022, China

[8]Max Planck Institute for Developmental Biology, Department of Molecular Biology, 72076 Tuebingen, Germany.

[9]Centre for Biological Systems Analysis, Albert-Ludwigs-University of Freiburg, Habsburgerstrasse 49, 79104 Freiburg, Germany.

[10]Freiburg Institute for Advanced Sciences (FRIAS), Albert-Ludwigs-University of Freiburg, Albertstrasse 19, 79104 Freiburg, Germany.

[11]BIOSS Centre for Biological Signalling Studies, Albert-Ludwigs-University of Freiburg, Schänzlestrasse 18, 79104 Freiburg, Germany.

[¥]Correspondence and request for material should be addressed to:

Franck A. Ditengou (franck.ditengou@biologie.uni-freiburg.de; Tel. +49 761 203 97 636) and Klaus Palme (klaus.palme@biologie.uni-freiburg.de; Tel. +49 761 203 29 54)

Word counts

Introduction: 697

Material and methods: 869

Results: 3151

Discussion: 1424

Acknowledgments: 118

Total Word count: 6259

Figures

Fig. 1- Color

Fig. 2- Color

Fig. 3- Color

Fig. 4- Color

Fig. 5

Fig. 6- Color

Fig. 7- Color

Summary

- Auxin gradients are sustained by series of influx and efflux carriers whose subcellular localization is sensitive to both exogenous and endogenous factors. Recently the localization of the *Arabidopsis thaliana* auxin efflux carrier PIN-FORMED (PIN) 6 was reported to be tissue specific and regulated though unknown mechanisms.
- Here, we used genetic, molecular and pharmacological approaches to characterize the molecular mechanism(s) controlling the subcellular localization of PIN6.
- PIN6 localizes to endomembrane domains in tissues with low *PIN6* expression levels such as roots, but localizes at the plasma membrane (PM) in tissues with increased *PIN6* expression such as the inflorescence stem and nectary glands. We provide evidence that this dual localization is controlled by PIN6 phosphorylation and demonstrate that PIN6 is phosphorylated by mitogen-activated protein kinases (MAPKs) MPK4 and MPK6. The analysis of transgenic plants expressing PIN6 at PM or in endomembrane domains reveals that PIN6 subcellular localization is critical for Arabidopsis inflorescence stem elongation post-flowering (bolting). In line with a role for PIN6 in plant bolting, inflorescence stems elongate faster in *pin6* mutant plants than in wild-type plants.
- We propose that PIN6 subcellular localization is under the control of developmental signals acting on tissue specific determinants controlling PIN6-expression levels and PIN6 phosphorylation.

Key words: *Arabidopsis thaliana,* auxin, bolting, inflorescence, stem

Introduction

Plant developmental plasticity involves the activity of series of plant hormones which modulate stem cell fate activity during plant development (Wolters & Jurgens, 2009; Rodriguez *et al.*, 2010). The plant hormone auxin plays a crucial role in this process as it coordinates the patterning of the plant body plan, including the establishment of apical–basal (Friml *et al.*, 2003), radial (Bjorklund *et al.*, 2007; Suer *et al.*, 2011; Ameres & Zamore, 2013), and proximal–distal axes (Sabatini *et al.*, 1999; Cai *et al.*, 2014) and the determination of cell fate by positional information (Ditengou *et al.*, 2008; Finet & Jaillais, 2012). Auxin is polarly transported by auxin influx and efflux carriers [(AUXIN RESISTANT 1/ Like AUX1 (AUX/LAX)) family (Ugartechea-Chirino *et al.*, 2010), ABCB/multi-drug resistance/P-glycoprotein (ABCB/MDR/PGP)(Paponov *et al.*, 2005; Geisler & Murphy, 2006), and PIN-FORMED (PIN) proteins (Paponov *et al.*, 2005)]. These proteins have been suggested to coordinate the patterning of the plant body plan (Sabatini *et al.*, 1999; Friml *et al.*, 2003; Bjorklund *et al.*, 2007; Ditengou *et al.*, 2008; Cai *et al.*, 2014).

PAT relies on the proper subcellular localization of PIN proteins. PIN1, PIN2, PIN3, PIN4 and PIN7 are targeted to the plasma membrane (PM) and they cycle between the PM and endosomal compartments (Geldner *et al.*, 2001). PIN8 localizes to the endoplasmic reticulum (ER) membranes (Mravec *et al.*, 2009; Dal Bosco *et al.*, 2012; Ding *et al.*, 2012; Simon *et al.*, 2016), while PIN5 and PIN6 localize to both the ER and PM (Ganguly *et al.*, 2014; Simon *et al.*, 2016). PIN5 was proposed to mediate auxin flow from the ER lumen to the cytosol (Mravec *et al.*, 2009), while PIN8 and PIN6 were proposed to export auxin in the opposite direction (Ganguly *et al.*, 2010; Dal Bosco *et al.*, 2012; Ding *et al.*, 2012). Together these studies suggest that PM-targeting of PIN-proteins probably depends on some tissue and/or cell specific determinants. Although it is unclear which mechanisms regulate PIN5 and PIN6 dual localization, it can be envisaged that PIN5 and PIN6 may be post-translationally modified prior their ultimate subcellular targeting, suggesting that these proteins are no longer recognized by the sorting machinery responsible for their retention in endomembrane domains. Phosphorylation is the most common post-translational modification involved in signal transduction. Three protein kinase families have been shown to phosphorylate PIN proteins: (i) D6 PROTEIN KINASE (D6PK) regulates auxin transport by phosphorylation of PIN1, PIN2, PIN3, PIN4 and PIN7 (Shen *et al.*, 2015); (ii) PINOID (PID) kinase and SERINE/THREONINE PROTEIN

PHOSPHATASE 2A (PP2A) antagonistically affect phosphorylation of the PIN hydrophilic loop, which is important for polar targeting of PM-located PIN proteins (Michniewicz *et al.*, 2007); and (iii) the recently characterized mitogen-activated protein kinase (MAPK) pathway, which consists of the MKK7-MPK6 complex that phosphorylates PIN1 serine 337 (S337) and impacts the polar localization of PIN1, thereby modifying shoot branching (Jia *et al.*, 2016).

In the present study, we aimed at characterizing the molecular mechanism(s) controlling PIN6 subcellular localization. Our study reveals that both *PIN6* gene expression level and PIN6 phosphorylation modulate PIN6 subcellular localization in Arabidopsis. Functional analysis of two phosphorylation sites, T392 and T393, which were reported to be phosphorylated *in vivo* in Arabidopsis suspension cells treated with bacterial elicitor flagellin (Benschop *et al.*, 2007), reveals that these sites play a key role in PIN6-ER exit and regulate root and root hairs growth, as well as inflorescence stem development. We demonstrate that PIN6 is phosphorylated by both MPK4 and MPK6 *in vitro*, although T393 is not phosphorylated by these kinases. Finally, the analysis of transgenic plants expressing PIN6 predominantly at PM or in ER reveals a critical role for PIN6 subcellular localization on inflorescence stem elongation post flowering. Hence, over-expressing a PIN6 mutant protein (T392V-T393V) that is retained in the ER-PIN6 does not affect inflorescence stem growth, while over-expressing native PIN6 or its PM-localized phosphomimetic mutant (T392E-T393E) drastically repressed plant growth and delayed bolting. In line with a role for PIN6 in plant bolting, the inflorescence stems elongated faster in *pin6* mutant plants than in wild-type plants. We conclude that PIN6 may act as a gate keeper ensuring that Arabidopsis plants efficiently develop the inflorescence stem at the appropriate, possibly environmentally determined time.

Materials and Methods

Materials and growth conditions

Arabidopsis thaliana (L.) Heynh. Columbia (Col-0) and *Landsberg erecta* (L*er*) ecotypes were used. All T-DNA insertion lines as well as transgenic lines are described in Methods S1. Seeds were surface sterilized and sown on solid Arabidopsis medium (AM) (2.3 g/L MS salts, 1% sucrose, 1.6% agar–agar, 5 mM 2-(N-morpholino)ethanesulfonic acid (MES) sodium salt (Sigma, Steinheim, Germany),

pH 6.0, adjusted with HCl). After vernalization for 2 days at 4°C, seeds were germinated under a long-day period (16 h light, 8 h darkness) at 22°C. The same growth conditions were applied in a phytochamber when plants were grown in soil.

Pharmacological treatments

For vesicular trafficking experiments, BFA (Invitrogen B7450) was used as previously described (Geldner *et al.*, 2001) with slight modifications: plants were incubated in 25 µM BFA (60 min). β-Estradiol was dissolved in 100% ethanol and added to AM without exceeding an ethanol concentration of 0.1%.

Free IAA level determination

Approximately 15 mg (fresh weight) of 5 mm root sections was homogenized and extracted for 16 h in methanol (Methods S2)

Generation of the PIN6 antibody

AtPIN6 cDNA (nucleotides 177-396) corresponding to the antigen peptide was inserted into the pET-28a(+) expression vector (Novagen). After expression in the *Escherichia coli* Rosetta strain (Novagen), the His6-tagged recombinant protein was affinity purified according to the Qiagen manual (Qiagen) and confirmed by SDS-polyacrylamide gel electrophoresis (PAGE). The antigen peptide included in the PAGE slice was used to immunize a rabbit (Eurogentec). The polyclonal antiserum was affinity purified against the recombinant AtPIN6 peptide as previously described (Hasumura *et al.*, 2005).

Detection of PIN6 by western blot

Proteins were extracted from 10, 3-week-old flower buds using extraction buffer containing 50 mM Tris-HCl, 10 mM EDTA, 2 mM EGTA, 0.1% SDS, 1 mM DTT, 10 µM protease inhibitor cocktail, 0.01 mM MG132 and 0.1 mM PMSF. After centrifugation at 10,000 rpm at 4°C for 15 min, the supernatant containing total protein was collected, and the protein concentration was measured using the Thermo Scientific Pierce Micro BCA Assay according to the manufacturer's instructions. After protein denaturation at 42°C in 5x Laemmli buffer (1:4), 7.4 mg/ml protein samples were separated on a 10% SDS-PAGE gel and then transferred to a nitrocellulose membrane. Blots were probed with a rabbit anti-PIN6 polyclonal antibody (1:1200), and PIN6 signal was detected with an HRP-conjugated anti-rabbit antibody (1:5000)

(Agrisera). Plasma membrane H^+-ATPase was used as a control for equal loading. Signal detection was performed with a Fujifilm ImageQuant™ LAS 4000 CCD camera using Super Signal West Pico Chemiluminescent substrate.

Immunolocalization

Plants were fixed with 4% paraformaldehyde in PBS (pH 7.3) and used for whole-mount *in situ* immunolocalization as previously described (Friml *et al.*, 2004).

Whole mount *in situ* hybridization

In situ detection of *PIN6* mRNA in Arabidopsis seedling root tips was performed as previously described (Riegler *et al.*, 2008; Begheldo *et al.*, 2013).

Quantitative RNA analysis

PIN6 expression was assessed using semi-quantitative RT-PCR (*PIN6* mRNA in 6-day-old PIN6ox plants) or qRT-PCR for PIN6 expression throughout the plant lifespan (Methods S4).

Microscopy and image post processing

Histological detection of β-glucuronidase (GUS) activity was performed as previously described (Scarpella *et al.*, 2004). Fluorescent proteins were analyzed as described in Methods S4. All images were assembled using Microsoft PowerPoint 2013.

Kinase assay

To test whether PIN6 in phosphorylated by MPK4 or MPK6, the hydrophilic loop (HL: residues 156-430) of PIN6 cDNA was amplified and cloned into pGEM-T Easy vector (Promega), and the sequence was verified. A non-phosphorylatable mutant HL version (T226A, T242A, S286A, T304A, T320A, S326A, S337A, and T393A; positions according to the full-length PIN6 protein) was synthetized by GenScript. The variant where T393 of the putative MAPK phosphosites is wild type was generated by inserting the sequence corresponding to A156-D352 from the mutant clone (including T226A, T242A, S286A, T304A, T320A, S326A and S337A) into the WT construct. For *in vitro* transcription/translation, the HL sequence variants were subcloned into the pEU3-NII-GLICNot vector with ligation-independent cloning (Bardoczy *et al.*, 2008). *In vitro* mRNA synthesis was carried out using a

TranscriptAid T7 High Yield Transcription Kit (Thermo Scientific) according to the manufacturer's instructions. Cell-free translation was completed using a WEPRO7240H Expression Kit (Cell Free Sciences, Japan). To activate His-tagged MPK4 and MPK6 when included in the phosphorylation assay solution, mRNA encoding constitutively active myc:MKK1 and myc:MKK4, respectively, were also added to the translation mixture as described (Nagy & Meszaros, 2014).

In vitro-translated His6-AtMPK4 and His6-AtMPK6 proteins were purified by affinity chromatography using TALON Magnetic Beads (Clontech), while *in vitro*-translated wild-type and mutant GST-PIN6loop variants were purified by affinity chromatography using Glutathione Magnetic Beads (Thermo Scientific)(Nagy & Meszaros, 2014). For kinase assays, 300 and 100 ng of *in vitro*-translated, affinity-purified substrate and kinase were used, respectively. As an activity control, 10 µg myelin basic protein (MBP) was used as a generic MAPK substrate (not shown). The assay was carried out in 20 mM HEPES, pH 7.5, 100 µM ATP, 1 mM DTT, 15 mM $MgCl_2$, 5 mM EGTA and 5 µCi [γ-^{32}P]ATP with bead-bound GST-PIN6loop variants as substrates for 30 min at room temperature and then stopped by the addition of Laemmli SDS buffer. Samples were fractionated by SDS-PAGE. The gel was fixed, stained with Coomassie blue, dried and analyzed by autoradiography.

Results

PIN6 expression level is variable and increases highly during plant bolting

PIN6 was reported to be located at the plasma membrane and in the ER in different cells and organs (Simon *et al.*, 2016), suggesting this dual localization may depend on some tissue and/or cell specific determinants. To gain insight on regulation of PIN6-localization, we first performed a quantitative RT-PCR analysis to ascertain *PIN6* expression throughout the Arabidopsis lifespan. As previously shown by qualitative *pPIN6:GUS* analysis (Nisar *et al.*, 2014), *PIN6* is expressed during both vegetative and reproductive plant growth phases (Fig. 1a) with highest *PIN6* mRNA levels in developing inflorescence stems (Fig. 1a). This observation was confirmed by analysis of *pPIN6::GUS* plants where *PIN6* expression was present in elongating inflorescence stems (Fig.Fig. S1b). These results are in agreement with publicly available data sets (Ismagul *et al.*, 2014; Ivanova *et al.*, 2014) and indicate that *PIN6* expression is under the control of developmental signals during bolting. Cross-sections from the inflorescence stem of *pPIN6:GUS* plants showed *PIN6* expression

in xylem parenchyma cells (Xpc), the fascicular cambium (Fc) and the interfascicular fiber tissues (IF) (Fig. S1f). Altogether, these observations show that *PIN6* is ubiquitously expressed during Arabidopsis life span. The fact that *PIN6* expression is increasing during plant bolting and stays relatively high in the stem, suggests a role of *PIN6* in processes controlling both longitudinal and radial differentiation, particularly during bolting.

PIN6 is localized at the PM in the shoot apical meristem, hypocotyl and inflorescence stem

To visualize PIN6 subcellular localization, we generated a polyclonal anti-PIN6 antibody. In agreement with a recent report (Simon *et al.*, 2016), PIN6 displayed dual localization in endomembrane domains and at the PM. We used the anti-PIN6 antibody to detect PIN6 at the root tip, the plant organ with the lowest *PIN6* expression levels. PIN6 was visible in the endomembrane compartments of the epidermis and cortex cell files (Fig. 1B), the tissues in which *PIN6* mRNA were low (Fig. 1a, Fig. S1E). However, in other tissues such as inflorescence stem vascular cells (Nisar *et al.*, 2014), vegetative leaves and flower primordia, which displayed higher *PIN6* mRNA levels, PIN6 was detected at the PM co-localized with PIN1 (Fig. 1a,c,d,f,g). To test the quality of the anti-PIN6 antibody, we performed both western blot analysis using the *pin6-5* mutant and immunolocalization using both the *pin6-5* and *pin6-6* mutants (Fig. S2b). PIN6 was recognized by the anti-PIN6 antibody in WT plants but as expected not in the mutants. This suggests that *pin6-5* and *pin6-6,* which were previously described as knock-down mutants at the mRNA level, are indeed null mutants at the protein level. This confirms that this antibody can be considered specific for PIN6. However, additional higher and lower molecular weight proteins were detected in both WT and *pin6-5* knock-out plants, which probably resulted in the background signals which were observed in the immunolocalization images (Fig. S2d-f, non-specific nuclear signals are indicated with an asterisk in WT and *pin6* knock-outs).

These data show that tissues with low *PIN6* expression display PIN6 in endomembrane domains, while PIN6 is at the PM in tissues with higher *PIN6* expression. This suggests that the dual localization of PIN6 may be dependent on *PIN6* expression level. To substantiate this correlation, we extended our analysis to other plant tissues reported to have strong *PIN6* expression, such as nectary glands

(Ludwig-Muller, 2014; Turi *et al.*, 2014). Observation of plants expressing the *pPIN6:GFP-PIN6* construct revealed that the GFP signal co-localized almost perfectly at the PM with the endosome tracker/PM-marker FM4-64 (Pearson's correlation coefficient in co-localized volume (PCCCV)=0.97, with a value of 1 representing a perfect correlation) (Fig. 2a-e). In contrast, very limited co-localization with the ER marker Rhodamine B (Zhang *et al.*, 2014) (PCCCV=0.26) was observed in both the median and lateral nectary glands (Fig. 2f-h). Taken together, these data support our hypothesis that the PM localization of PIN6 most likely depends on the *PIN6* expression level. Analysis of the PIN6-subcellular localization in nectary glands also revealed basally (toward the root) localized GFP-PIN6, presumably exporting auxin out of nectary glands, thus supporting the idea that nectary glands could be potential sources of auxin (Aloni *et al.*, 2006) (Fig. 2i,j).

PIN6 is targeted to the PM upon *PIN6* overexpression

To confirm the relationship between *PIN6* expression level and PIN6 subcellular localization, we generated transgenic lines overexpressing the *PIN6* genomic sequence with (*GFP-PIN6ox*) or without (PIN6ox) a *GFP* tag and driven by the constitutively active *CaMV35S* promoter. The non-tagged construct was used to confirm that GFP does not affect PIN6 sub-cellular localization. We visualized PIN6 subcellular localization in *GFP-PIN6ox* and *PIN6ox* plants and analyzed its impact on root and shoot growth. *PIN6* overexpression increased the *PIN6* mRNA level and thus the PIN6 protein level (Fig.3a and Fig. S2b); both GFP-tagged and non-tagged PIN6 were detected at the PM, where they co-localized with FM4-64 (PCCCV=0.7) (Fig. 3e-h). In line with recent studies (Ganguly *et al.*, 2010; Cazzonelli *et al.*, 2013; Simon *et al.*, 2016), the roots of both GFP-*PIN6ox* and *PIN6ox* plants were hairless and displayed a strong waving phenotype, suggesting that GFP insertion did not affect PIN6 functionality (Fig. 3b-d). More thorough inspection of the PIN6 sub-cellular localization showed that PM-located PIN6 (PM-PIN6) exhibited polar localization in root cells similar to our observations in nectary glands (see above). In the cortex and stele cells, PIN6 co-localized basally with PIN1 (Fig. 3i and Fig. S3a). The PIN6 PM-localization was most striking in the epidermis For clarity, the epidermis cell file of the root meristematic zone was divided into two tiers (see Fig. 3i). Epidermal cell tier 1 represents cells located in the upper part of the meristematic zone, while tier 2 represents the lower part. The oldest cell of the most recent lateral

root cap cells (LRC) (solid white forward arrow in Fig. 3i) marks the limit between the two tiers. In tier 1, PIN6 localized apically (toward the shoot) similarly to PIN2, with a well-defined polarity in cells destined to elongate (Fig. 3i and Fig. S3b). In contrast, in tier 2, PIN6 localized laterally and basally, pointing progressively towards the quiescent centre (QC) and columella cells and presumably channeling auxin towards this region (Fig. 3i and Fig. S3a). Indeed, PM-localized PIN6 perturbed auxin distribution in PIN6ox roots as confirmed by both quantification of auxin levels and the expression of the auxin-sensitive *DR5::GUS* reporter fusion protein at the *PIN6ox* root tip (Fig. S3e-g) (Cazzonelli *et al.*, 2013).

PID regulates PIN6 polarity despite altered phosphosite occurrence

The unique localization dynamics of PIN6 suggests that it is under the control of a unique regulatory mechanism. Phosphorylation has been already shown to be a key determinant of PIN localization, the best characterized mechanism is the regulation of PIN polarity by members of the AGCVIII protein kinase subfamily, PID and D6PK and their close paralogues. The main D6PK site of PIN1 (S271) is conserved in all long-HL PINs, including PIN6 (S291) (Zourelidou *et al.*, 2014). The three PID phosphorylation sites are similarly well conserved in long-HL PINs with the exception of PIN6, where the site corresponding to S252 of PIN1 is missing. Although PID is known to regulate polarity, not localization to the PM, we first tested whether this differential PID site composition can be associated with a differential regulation of PIN6 by PID. In *PIDox* plants, PIN1 polarity was shifted from the basal to the apical side in the stele (Friml *et al.*, 2004), whereas the cytoplasmic localization of PIN6 in epidermal cells remained unchanged, implying that PID does not bring about PM translocation of PIN6 (Fig. S5a-c) (Friml *et al.*, 2004; Rasmussen *et al.*, 2015). Furthermore, we crossed PIN6 overexpression (*PIN6ox*) and *PINOID*-overexpression (*PIDox*) plant materials. Similarly to PIN6ox plants, PIN6 was localized to PM in *PIDoxPIN6ox* plants, but the PM-PIN6 basal localization in the stele shifted, similarly to PIN1 (Fig. S5g-i). Moreover, the basal localization of PM-PIN6 in tier 2 epidermal cells also shifted, whereas the apical localization of PIN6 in tier 1 epidermal cells did not (in 100% of plants tested, n>15; compare Fig. 3i and Fig. S5d-f with Fig. S5g-i). These results imply that similarly to other PINs, PID plays a role in polarity regulation of PIN6, however its ER to PM translocation is regulated by other means.

Threonine-phosphorylation sites 392 (T392) and 393 (T393) are involved in PIN6 localization at the PM

A phosphoproteomic assay in Arabidopsis yielded PIN6 phosphopeptides from suspension-cell-derived PM vesicles (Benschop *et al.*, 2007). In that study, PM-localised PIN6 protein was shown to be phosphorylated at both or either of the two adjacent threonine residues at positions T392 and T393 in the hydrophilic loop (Benschop *et al.*, 2007). These phosphorylation sites are partially conserved among PIN6-like proteins in other species (Fig. S6b). Remarkably, these residues are not conserved in other members of the PIN family (Fig. S6b), raising the possibility of a PIN6-specific regulation through their phophorylation. In order to test this hypothesis both T392 and T393 were converted by site-directed mutagenesis to valine, an amino acid that cannot be phosphorylated (PIN6^{T392EVT393V}) or to glutamic acid, which mimics constitutive phosphorylation (PIN6$^{T392E/T393E}$). Driven by a β-estradiol-inducible promoter, the intact *PIN6* gene (*PIN6ox-i*) and the mutated versions were separately introduced into WT plants. When grown in the presence of β-estradiol, the roots of *PIN6ox-i* and PIN6$^{T392E/T393E}$ plants were dramatically affected in comparison to the roots of WT and PIN6$^{T392V/T393V}$ plants (Fig. 4a-d, top panel). *PIN6ox-i* and PIN6$^{T392E/T393E}$ plants developed hairless agravitropic roots (Fig. 4a-d, middle panel). Consistent with this, confocal microscope images revealed that, as for *PIN6ox* plants (Fig. 3i), PIN6 localized basally at the PM in *PIN6ox-i* root tip epidermal cells (Fig. 4b, lower panel). In PIN6$^{T392E/T393E}$ plants, the GFP signal also localized to the PM but was non-polar (Fig. 4c, lower panel; Video S1). Altogether, these data indicate that the presence of PIN6 at the PM of epidermal cells, and not necessarily its polarity, is sufficient to perturb both the root gravity response and root hair development. In contrast, PIN6$^{T392V/T393V}$ plants were indistinguishable from WT plants, and the GFP signal was mainly visible in the ER, where it co-localized with the ER marker rhodamine B hexyl (PCCCV=0.65) (Fig. 4d and Fig. S7a; Video S2). It is known that PM-localized PINs are sensitive to the fungal toxin brefeldin A (BFA), which blocks PIN protein recycling, while ER-PINs are BFA resistant (Mravec *et al.*, 2009). Accordingly, upon BFA treatment, PIN6$^{T392E/T393E}$ co-localized with FM4-64 in BFA compartments, while PIN6$^{T392V/T393V}$ localization was not affected, thus confirming their respective subcellular localizations (Fig. S7b-c). These data demonstrate that T392 and T393 phosphorylation sites are crucial the translocation of PIN6 to the PM.

PIN6 hydrophilic loop is phosphorylated by MPK4 and MPK6 but T393 is not a MAP kinase phosphorylation site

In order to predict putative kinase(s), which may mediate T392/T393 phosphorylation, we screened the PIN6 protein sequence by using the Eukaryotic Linear Motif (ELM) database (Dinkel *et al.*, 2016). This search resulted in a total of 59 predicted phosphorylation sites targeted by eight types of kinases. In the region of interest T393 was identified as a MAPK phosphorylation site, while no putative kinase was associated with T292. T393 is one of eight potential proline-directed MAPK phosphorylation sites in PIN6 HL (T226, T242, S286, T304, T320, S326, S337, and T393) suggesting that PIN6 may be phosphorylated by MAP-kinase(s). In plants, MAPK pathways are central regulators of various stress responses and developmental processes (Rodriguez *et al.*, 2010; Xu & Zhang, 2015). In particular, MPK6 of Arabidopsis, the best studied plant MAP kinase, has been reported to specifically regulate developmental processes such as lateral root development and plant height (Jia *et al.*, 2016), processes also shown to be altered in *pin6* mutants (Cazzonelli *et al.*, 2013; Simon *et al.*, 2016). MPK4, another well-characterized plant MAPK is involved in defense regulation, with *mpk4* mutants displaying severe dwarfism and altered cell division and microtubule dynamics. Based on this information we first tested whether PIN6 is phosphorylated by MPK4 and MPK6 using *in vitro* kinase assays (Fig. 5).

The incorporation of radiolabeled phosphate in the hydrophilic loop (HL) of PIN6 in the presence of activated MPK4 or MPK6 indicates that this protein is phosphorylated by both kinases (Fig. 5). As a negative control, all eight MAPK phosphorylation residues (S or T) were replaced with the non-phosphorylatable amino acid alanine (T226A, T242A, S286A, T304A, T320A, S326A, S337A, and T393A in PIN6-mut8), which results in the loss of MAPK-mediated phosphorylation (Fig. 5). Faint, residual phosphorylation of the mutant proteins by MPK6 indicates weak, unspecific phosphorylation on non-cognate residues, probably related to the strong activity of MPK6. These results confirm MAPK-mediated phosphorylation of PIN6. In order to test whether T393 is one of the residues actually phosphorylated by these MAPKs we tested specific phosphorylation of T393 by using a septuple mutant, where T393 is wild type (i.e. T226A, T242A, S286A, T304A, T320A, S326A, S337A; PIN6-mut7). Neither MPK4 nor MPK6 phosphorylated PIN6 on T393 (Fig. 5), suggesting that this residue is not a genuine MAP kinase site. These data reveal complex regulation of

PIN6 by at least two MAPK pathways, but also indicate that the modification of T392/T393 regulating PIN6 PM translocation is probably brought about by yet another type of protein kinase.

PM-localized PIN6 represses plant growth

To investigate the importance of PIN6 subcellular localization on plant development, we analyzed the phenotype of PIN6$^{T392E/T393E}$ and PIN6$^{T392V/T393V}$ plants grown in soil. Spraying plants with 100 µM ß-estradiol affected weakly the growth of Col-0 and PIN6$^{T392E/T393E}$ plants, but strongly retarded the growth of PIN6$^{T392E/T393E}$ and PIN6ox-i plants (Fig. S8a, b). Plants sprayed with water showed a similar elongation profile for the inflorescence stems of Col-0 and PIN6$^{T392V/T393V}$, while PIN6$^{T392E/T393E}$ plants developed significantly smaller inflorescences. This result confirms the reported leakiness of the estradiol-inducible promoter (Kubo *et al.*, 2013), as indicated by the GFP signal observed in the leaves of non-induced PIN6$^{T392V/T393V}$ and PIN6$^{T392E/T393E}$ plants (Fig. S8c). ß-estradiol also affected weakly the growth of Col-0 and PIN6$^{T392V/T393V}$ plants, but it strongly delayed the growth of PIN6$^{T392E/T393E}$ inflorescence stems and completely suppressed the bolting of PIN6ox-i plants (Fig. S8d). Taken together, these data demonstrate the importance of T392 and T393 for the regulation of plant inflorescence stem elongation and indicate that the phosphorylation-dependent PM targeting of PIN6 negatively controls inflorescence stem development, while preventing this phosphorylation results in the ER retention of PIN6. These data also suggested a role for PIN6-dependent auxin distribution during the elongation of the inflorescence stem.

Inflorescence stem elongation is accelerated in *pin6* loss-of-function mutants

In *Arabidopsis thaliana*, the floral transition (formation of an inflorescence meristem) marks the transition from the vegetative to the reproductive phase followed by elongation of the first internode, known as the bolting transition (Pritchard *et al.*, 2012). This process is influenced by hormones but underlying mechanisms still remain poorly understood. To explore how PIN6-dependent PAT modulates inflorescence stem development, we analyzed the *pin6-5* (GK-430B01) and *pin6-6* (GK-711C09) T-DNA insertion lines (Supporting Information Fig. S2A; (Cazzonelli *et al.*, 2013). We also analyzed two additional novel knock-out lines isolated from the Arabidopsis Genetrap collection in the *Landsberg erecta* (L*er*) background

(Sundaresan *et al.*, 1995) (referred to here as *pin6-7* (GT7129) and *pin6-8* (GT6906)), in which T-DNA is inserted in the 4th and 5th introns, respectively (Supporting Information Fig. S2C). All *pin6* mutants developed inflorescence stems 3-5 times longer than wild-type (WT) inflorescence stems while having the same number of leaves. This phenotype suggests faster inflorescence stem elongation rather than early flowering (Fig. 6a-d).

PIN6 overexpression delays inflorescence stem elongation

In contrast to *pin6* mutants and in line with previously published phenotypes (Cazzonelli *et al.*, 2013), plants overexpressing *PIN6* developed significantly shorter inflorescence stems (Fig. 6d). Compared to WT plants, these plants developed siliques relatively close to the base of the inflorescence stem (indicated with an arrow in Fig. S9a), suggesting that these plants were mature and capable of seed production but that inflorescence stem elongation was arrested (Fig. 6a-d). To confirm these results, we quantified the flowering time and the growth rates of WT, *pin6-5* and *pin6-5* complemented with GFP-PIN6 driven by the *PIN6* native promoter (*pPIN6:PIN6:GFP*). In our conditions, all plants (WT, *pPIN6:PIN6-GFP*, *pin6-5*, and *PIN6ox*) flowered around the 28th day after sowing (DAS). However, although the apical flower was visible in PIN6ox and GFP-PIN6ox plants, inflorescence stem elongation required four additional days (Fig. 6e). WT and *pin6-5 pPIN6:PIN6-GFP* plants displayed accelerated growth starting on the 34th day (open arrow in Fig. 6e), but this acceleration occurred earlier in *pin6-5* plants (closed arrow in Fig. 6e). Thus, six days after bolting, the growth rate of *pin6-5* mutant inflorescences was approximately 2.42 cm/day versus 1.65 and 1.43 cm/day for WT and *pin6-5 pPIN6:PIN6-GFP* plants, respectively (Fig. S9b), demonstrating the rapid growth of pin6-5 plants and mutant complementation by the *pPIN6:PIN6-GFP* construct. Conversely, GFP-PIN6ox and PIN6ox inflorescence stem elongation was slower (only 0.25 and 0.13 cm/day, respectively (Fig. S9b)). The data also indicated that the accelerated growth of *pin6* mutants is transient. Later, the WT and *pin6-6* mutant (a trend visible in all mutants; not shown) growth rates became equal, while the PIN6ox growth rate remained approximately 50% lower (Fig. S9c,d). Taken together, these data demonstrate that PIN6 activity regulates inflorescence stem elongation and strongly suggest a role for auxin transport during plant bolting.

Auxin response is reduced in *pin6* mutants

Auxin transport capacities and auxin levels are crucial for shoot branching and vascular tissue development (Muller & Leyser, 2011; Peer *et al.*, 2011; Bennett *et al.*, 2014). For example, a cambial auxin peak resulting from basipetally derived shoot-apex auxin is essential for both primary and secondary growth (Bjorklund *et al.*, 2007; Suer *et al.*, 2011; Ameres & Zamore, 2013). To determine how PIN6 activity modulates auxin distribution and levels in bolting inflorescences, we used a *pDR5:GFP* reporter (Ottenschlager *et al.*, 2003) to visualize auxin distribution and activity in inflorescence stems six days after bolting. In transverse sections 50 mm above the uppermost rosette leaf of the inflorescence stem of WT plants, the DR5:GFP signal was mainly visible in phloem and xylem parenchyma cells (Fig. 7a,f,i). The DR5 signal was significantly lower in the *pin6-5* mutant (T-test, $P<0.05$, n=10); in contrast, DR5 expression was significantly greater in *PIN6ox* plants (T-test, $P<0.001$, n=10) (Fig. 7b-d). In addition, radial development was reduced in *PIN6ox* plants but increased in *pin6-5* plants (Fig. 7b-e). Consequently, *pin6-5 DR5:GFP* plants displayed a greater transversal stem surface area than *DR5:GFP* and *PIN6oxDR5:GFP* plants (T-test, $P<0.001$, n=10). In *PIN6ox DR5:GFP* plants, the number of xylem elements was significantly reduced and accompanied by ectopic development of xylem parenchyma cells (Fig. 7f-l; xylem parenchyma cells are indicated with a white arrow in Fig. 7i and k). Altogether, these data establish *PIN6* as a key regulator of both the primary and secondary growth of Arabidopsis inflorescence stems and show that impaired PIN6 activity strongly affects the auxin response necessary for cambium proliferation and xylem differentiation (Hildebrandt & Nellen, 1992; Nina Theis & Manuel Lerdau, 2003; Suer *et al.*, 2011).

Discussion

Previous studies revealed the importance of the auxin transporter PIN6 in several developmental processes, such as nectary development (Bender *et al.*, 2013), leaf vein patterning (Sawchuk *et al.*, 2013), and root and lateral root development (Cazzonelli *et al.*, 2013; Simon *et al.*, 2016). Recently, Simon and colleagues described the PM and ER subcellular localization of PIN6 and suggested its role in controlling auxin transport and homeostasis in auxin-mediated development (Simon

et al., 2016). In the present study, using genetic, molecular and pharmacological approaches, we characterized the mechanisms controlling PIN6 dual localization and uncovered a role for PIN6 during Arabidopsis inflorescence stem development.

PIN6 subcellular localization is regulated by *PIN6* gene expression levels

It was reported that auxin can induce the *PIN6* promoter in a tissue-specific manner (Cazzonelli *et al.*, 2013). Hence when combined to the finding that high *PIN6* expression results in PM-targeting of PIN6, it is not surprising to find PIN6 expressed at the PM in tissues reported to contain high levels of auxin such as the tip of young leaves, young flowers, vascular tissue of the stem and nectary glands (Muller *et al.*, 2002; Benkova *et al.*, 2003; Aloni *et al.*, 2006; Cheng *et al.*, 2006). We did not observe PIN6 at the PM of root cells, despite the fact that auxin is synthesized and accumulates at the root tip. This suggests that at the root tip, besides auxin levels other cell determinants probably modulate PIN6 abundance and therefore its localization. In contradiction with our data, GFP-tagged PIN6 driven by the *PIN6* native promoter was recently reported to localize at the PM in the Arabidopsis root tip (Simon *et al.*, 2016), although whether this construct could rescue the described mutant phenotypes is not presented in that paper.

T392/T393 phosphorylation sites modulate PIN6 subcellular localization

PINOID (PID) kinase and SERINE/THREONINE PROTEIN PHOSPHATASE 2A (PP2A), were reported to be involved in the reversible phosphorylation of the PIN hydrophilic loop (Michniewicz *et al.*, 2007), although it is still unclear how PID regulates PIN trafficking (New ref), Nevertheless. our data indicate that despite loss of a PID site PIN6 retains a similar sensitivity to PID-dependent phosphorylation as PIN1, i.e. PIN6 basal localization is flipped to apical localization. However, we have no evidence that PID activity is responsible for PIN6 exit from the ER, since PIN6 is not targeted to PM in PIDox plants, since PIN6 is not targeted to the PM in 35S::PID plants; instead this observation indicates a role for other kinases.

Data mining retrieved *in vivo* phosphorylation at a tandem threonine pattern (T392/T393) unique to PIN6. Accordingly, functional analyses confirmed that the T392 and T393 residues are crucial for PIN6 ER exit and subsequent PM localization. In line with this, genetic modifications preventing phosphorylation of these residues resulted in PIN6 retention in the ER. A similar mechanism was

described for the PM-targeting of Arabidopsis PHOSPHATE TRANSPORTER1 (PHT1) (Bayle *et al.*, 2011), the nitrate transporter and auxin facilitator NRT1.1 (Krouk *et al.*, 2010; Habets & Offringa, 2014) and the aquaporin PIP2;1 (Weiste & Droge-Laser, 2014). Phosphorylation of these proteins was shown to modulate their targeting to the PM.

PIN6 is phosphorylated by MPK4 and MPK6

Phosphorylation of PIN6 at T392/T393 represents a novel regulatory mechanism, thus we set out to identify the corresponding kinase(s). As there are 942 kinases encoded in the Arabidopsis genome (Zulawski *et al.*, 2014), *in silico* pattern screening appeared to be the feasible approach to predict the kinase(s) phosphorylating T392 and/or T393. Accordingly, T393 is one of eight putative MAP kinase phosphorylation sites in PIN6 HL. Here we provide evidence that PIN6 is phosphorylated by both MPK4 and MPK6, thus revealing a novel regulatory mechanism, although T393 is not phosphorylated by MPK4 or MPK6. Preference of MAP kinases towards specific residues within a set of potential phosphosites has been precedented in case of other substrates, e.g (Furlan *et al.*, 2017). Thus the identity of the kinase(s) phosphorylating T392 and/or T393 remains elusive in light of current kinase analysis tools. MAP kinases are involved in several adaptive and developmental processes controlled by environmental stress (Pitzschke *et al.*, 2009; Rodriguez *et al.*, 2010; Xu & Zhang, 2015). In particular, MKK7 is a repressor of PAT (Dai *et al.*, 2006), and the MKK7-MPK6 cascade was recently shown to be involved in PAT and to have a direct impact on auxin distribution in inflorescence stems (Jia *et al.*, 2016). MPK4 is known to modulate plant defense and development (Petersen *et al.*, 2000; Gawronski *et al.*, 2014). In light of MAPK-mediated phosphorylation of two PINs and the involvement of two MAPK pathways [(Jia *et al.*, 2016); this study], a complex regulatory network is emerging, which suggests an adaptive growth mechanism allowing plants to rapidly respond to environmental or developmental changes and fits well with the central role of MAPK pathways in adaptive regulation. For this respect, *in vivo* analysis of PIN6 phosphorylation by MPK4 or MPK6 in response to various stresses will be very informative.

PIN6-depedent auxin transport regulates inflorescence stem elongation

Our data show that *PIN6* expression is regulated by both developmental and tissue-specific determinants throughout the entire plant lifespan. *PIN6* expression does not regulate the transition to flowering, as flowering time in terms of leaf number at the onset of bolting is unaltered in both *pin6* and *PIN6ox* genotypes. Therefore, PIN6-dependent auxin transport is crucial for inflorescence stem elongation after floral initiation. The significance of PIN6-mediated auxin transport in inflorescence stem development is related to the degree of *PIN6* expression. Ectopic expression of PIN6 in *PIN6ox* plants causes the auxin accumulation (Cazzonelli *et al.*, 2013) responsible for inhibiting inflorescence stem elongation, while lower auxin levels in the *pin6* mutant promote both radial extension and faster inflorescence stem elongation. This is in line with the well-accepted result that perturbing PAT alters the normal development of Arabidopsis inflorescence stems (Okada *et al.*, 1991; Wilson *et al.*, 2013) and with the reported auxin concentration-dependent effect on stem elongation, in which the application of high concentrations of auxin directly inhibits the growth of shoots, while lowering auxin concentrations promotes growth (Thimann, 1939). It is possible that PIN6-dependent auxin gradients differentially regulate the genes controlling cell expansion, thus inhibiting cell growth when auxin levels are high, such as occurs in *PIN6ox* plants.

By delaying elongation of the inflorescence stem, PIN6-dependent auxin transport allows the plant to optimally mature, hence optimizing seed yields. On the other hand, lowering *PIN6* function appears to be a relevant tool for accelerating or delaying inflorescence stem development. We propose that PIN6 acts as a gate keeper, ensuring that Arabidopsis plants efficiently develop the inflorescence stem at the appropriate, environmentally determined time and that inflorescence stem development is timed in accordance with environmental conditions. The underlying regulatory mechanisms probably involve upstream factors that sense environmental changes and activate the kinases that phosphorylate PIN6, thereby stimulating its exit from the ER. In this respect, it is remarkable that MAPK signaling is activated by various environmental signals.

The fact that inflorescence stem elongation is repressed in plants overexpressing *PIN6* [this study; (Cazzonelli *et al.*, 2013)] and in PIN6$^{T392E/T393E}$ plants, where PIN6 localizes at the PM, suggests the existence of a correlation between PIN6 phosphorylation status, the PM-localization of PIN6 and the elongation of the inflorescence stem during plant bolting. PM localization of PIN6 is crucial, as it may

contribute to the fine tuning of the tissue-specific auxin amounts necessary for the optimal development of the Arabidopsis inflorescence stem. Furthermore, although PIN6 is an auxin efflux carrier (Petrasek *et al.*, 2006; Simon *et al.*, 2016), its activity once targeted to the PM is quite intriguing, particularly in relation to the other PM-localized PIN proteins. The *pin1* mutant displays several developmental defects such as naked, pin-shaped inflorescences (Galweiler *et al.*, 1998) and delayed bolting *(Okada et al., 1991; Galweiler et al., 1998)*, whereas *35S::PIN1* plants bolt similarly to WT (Benkova *et al.*, 2003). In comparison, *pin6* mutants bolt faster, while PIN6ox plants are severely delayed. Since PIN6 and PIN1 both localize to the PM in WT stems, it is logical that their combined basipetal auxin transport activities are required for inflorescence stem development. Interestingly, PAT was shown to be increased in *35S::PIN1* plants but significantly reduced in plants overexpressing *PIN6* (Cazzonelli *et al.*, 2013). Altogether, these observations suggest that PIN6 and PIN1 probably have distinct activities during inflorescence stem development.

Taken together, our data suggest a mechanism in which environmental/developmental cues act at both the transcriptional and posttranscriptional levels by stimulating *PIN6* expression and inducing the phosphorylation and subsequent translocation of PIN6 protein to the PM (Fig. S10).

Acknowledgements

This work could not have been accomplished without the help of colleagues, collaborators and friends who provided support, suggestions and materials. We gratefully acknowledge the excellent technical support from Beata Ditengou, Khushbu Singh and Jean Hubschwerlin. This work was supported by the Baden-Württemberg Stiftung, Deutsche Forschungsgemeinschaft (SFB 746, INST 39/839,840,841), the Excellence Initiative of the German Federal and State Governments (EXC 294), Bundesministerium für Forschung und Technik (BMBF 0315329B, 0315690A, 0316185B), Deutsches Zentrum für Luft und Raumfahrt (DLR 50WB1022), the Hungarian Research Fund (OTKA K101250, NN114511, NN111085), the National Natural Science Foundation of China (31320103910 and 31570291) and the National Basic Research Program of China (2015CB942900). RD is a Bolyai Fellow of the Hungarian Academy of Sciences.

Author contributions

F.A.D., H.N., P.K., C.L., T. M., R.D. and K.P. conceived and designed the experiments. F.A.D., D.G., H.N., P.K., H.L., V.M., I.P., K.R., L.Q., X.L., C.B., S.N., and T.V.N. performed the experiments. F.A.D., H.N., P.K., C.L., T. M., B.B., R.D. and K.P. analyzed the data. F.A.D. wrote the paper. All authors discussed the results and commented on the manuscript.

References

Aloni R, Aloni E, Langhans M, Ullrich C. 2006. Role of auxin in regulating Arabidopsis flower development. *Planta* **223**: 315 - 328.

Ameres SL, Zamore PD. 2013. *Nature Rev. Mol. Cell Biol.* **14**: 475-488.

Bardoczy V, Geczi V, Sawasaki T, Endo Y, Meszaros T. 2008. A set of ligation-independent in vitro translation vectors for eukaryotic protein production. *Bmc Biotechnology* **8**.

Bayle V, Arrighi JF, Creff A, Nespoulous C, Vialaret J, Rossignol M, Gonzalez E, Paz-Ares J, Nussaume L. 2011. Arabidopsis thaliana High-Affinity Phosphate Transporters Exhibit Multiple Levels of Posttranslational Regulation. *Plant Cell* **23**(4): 1523-1535.

Begheldo M, Ditengou FA, Cimoli G, Trevisan S, Quaggiotti S, Nonis A, Palme K, Ruperti B. 2013. Whole-mount in situ detection of microRNAs on Arabidopsis tissues using Zip Nucleic Acid probes. *Anal Biochem* **434**(1): 60-66.

Bender RL, Fekete ML, Klinkenberg PM, Hampton M, Bauer B, Malecha M, Lindgren K, A. Maki J, Perera MADN, Nikolau BJ, et al. 2013. PIN6 is required for nectary auxin response and short stamen development. *The Plant Journal* **74**(6): 893-904.

Benkova E, Michniewicz M, Sauer M, Teichmann T, Seifertova D, Jurgens G, Friml J. 2003. Local, efflux-dependent auxin gradients as a common module for plant organ formation. *Cell* **115**(5): 591-602.

Bennett T, Hines G, Leyser O. 2014. Canalization: what the flux? *Trends in Genetics* **30**(2): 41-48.

Benschop JJ, Mohammed S, O'Flaherty M, Heck AJ, Slijper M, Menke FL. 2007. Quantitative phosphoproteomics of early elicitor signaling in Arabidopsis. *Mol Cell Proteomics* **6**(7): 1198-1214.

Bjorklund S, Antti H, Uddestrand I, Moritz T, Sundberg B. 2007. Cross-talk between gibberellin and auxin in development of Populus wood: gibberellin stimulates polar auxin transport and has a common transcriptome with auxin. *Plant Journal* **52**(3): 499-511.

Cai XT, Xu P, Zhao PX, Liu R, Yu LH, Xiang CB. 2014. Arabidopsis ERF109 mediates cross-talk between jasmonic acid and auxin biosynthesis during lateral root formation. *Nature Communications* **5**: 5833.

Cazzonelli CI, Vanstraelen M, Simon S, Yin K, Carron-Arthur A, Nisar N, Tarle G, Cuttriss AJ, Searle IR, Benkova E, et al. 2013. Role of the Arabidopsis PIN6 Auxin Transporter in Auxin Homeostasis and Auxin-Mediated Development. *PLoS One* **8**(7): e70069.

Cheng Y, Dai X, Zhao Y. 2006. Auxin biosynthesis by the YUCCA flavin monooxygenases controls the formation of floral organs and vascular tissues in Arabidopsis. *Genes Dev* **20**(13): 1790-1799.

Dai Y, Wang HZ, Li BH, Huang J, Liu XF, Zhou YH, Mou ZL, Li JY. 2006. Increased expression of MAP KINASE KINASE7 causes deficiency in polar auxin transport and leads to plant architectural abnormality in Arabidopsis. *Plant Cell* **18**(2): 308-320.

Dal Bosco C, Dovzhenko A, Liu X, Woerner N, Rensch T, Eismann M, Eimer S, Hegermann J, Paponov IA, Ruperti B, et al. 2012. The endoplasmic reticulum localized PIN8 is a pollen-specific auxin carrier involved in intracellular auxin homeostasis. *Plant Journal* **71**(5): 860-870.

Ding Z, Wang B, Moreno I, Duplakova N, Simon S, Carraro N, Reemmer J, Pencik A, Chen X, Tejos R, et al. 2012. ER-localized auxin transporter PIN8 regulates auxin homeostasis and male gametophyte development in Arabidopsis. *Nature Communications* **3**: 941.

Dinkel H, Van Roey K, Michael S, Kumar M, Uyar B, Altenberg B, Milchevskaya V, Schneider M, Kuhn H, Behrendt A, et al. 2016. ELM 2016--data update and new functionality of the eukaryotic linear motif resource. *Nucleic Acids Res* **44**(D1): D294-300.

Ditengou FA, Tealea WD, Kochersperger P, Flittner KA, Kneuper I, van der Graaff E, Nziengui H, Pinosa F, Li X, Nitschke R, et al. 2008. Mechanical induction of lateral root initiation in Arabidopsis thaliana. *Proceedings of the National Academy of Sciences of the United States of America* **105**(48): 18818-18823.

Finet C, Jaillais Y. 2012. AUXOLOGY: When auxin meets plant evo-devo. *Developmental Biology* **369**(1): 19-31.

Friml J, Vieten A, Sauer M, Weijers D, Schwarz H, Hamann T, Offringa R, Jurgens G. 2003. Efflux-dependent auxin gradients establish the apical-basal axis of Arabidopsis. *Nature* **426**(6963): 147-153.

Friml J, Yang X, Michniewicz M, Weijers D, Quint A, Tietz O, Benjamins R, Ouwerkerk PB, Ljung K, Sandberg G, et al. 2004. A PINOID-dependent binary switch in apical-basal PIN polar targeting directs auxin efflux. *Science* **306**(5697): 862-865.

Furlan G, Nakagami H, Eschen-Lippold L, Jiang X, Majovsky P, Kowarschik K, Hoehenwarter W, Lee J, Trujillo M. 2017. Changes in PUB22 Ubiquitination Modes Triggered by MITOGEN-ACTIVATED PROTEIN KINASE3 Dampen the Immune Response. *Plant Cell*.

Galweiler L, Guan C, Muller A, Wisman E, Mendgen K, Yephremov A, Palme K. 1998. Regulation of polar auxin transport by AtPIN1 in Arabidopsis vascular tissue. *Science* **282**: 2226-2230.

Ganguly A, Lee SH, Cho M, Lee OR, Yoo H, Cho H-T. 2010. Differential Auxin-Transporting Activities of PIN-FORMED Proteins in Arabidopsis Root Hair Cells. *Plant Physiology (Rockville)* **153**(3): 1046-1061.

Ganguly A, Park M, Kesawat MS, Cho HT. 2014. Functional Analysis of the Hydrophilic Loop in Intracellular Trafficking of Arabidopsis PIN-FORMED Proteins. *Plant Cell* **26**(4): 1570-1585.

Gawronski P, Witon D, Vashutina K, Bederska M, Betlinski B, Rusaczonek A, Karpinski S. 2014. Mitogen-activated protein kinase 4 is a salicylic acid-independent regulator of growth but not of photosynthesis in Arabidopsis. *Mol Plant* **7**(7): 1151-1166.

Geisler M, Murphy AS. 2006. The ABC of auxin transport: the role of p-glycoproteins in plant development. *FEBS Lett* **580**(4): 1094-1102.

Geldner N, Friml J, Stierhof YD, Jurgens G, Palme K. 2001. Auxin transport inhibitors block PIN1 cycling and vesicle trafficking. *Nature* **413**(6854): 425-428.

Habets ME, Offringa R. 2014. PIN-driven polar auxin transport in plant developmental plasticity: a key target for environmental and endogenous signals. *The New phytologist* **203**(2): 362-377.

Hasumura M, Imai T, Takizawa T, Ueda M, Onose J, Hirose M. 2005. Promotion of thyroid carcinogenesis by para-aminobenzoic acid in rats initiated with N-bis(2-hydroxypropyl)nitrosamine. *Toxicological Sciences* **86**(1): 61-67.

Hildebrandt M, Nellen W. 1992. Differential antisense transcription from the Dictyostelium EB4 gene locus: implications on antisense-mediated regulation of mRNA stability. *Cell* **69**(1): 197-204.

Ismagul A, Iskakova G, Harris JC, Eliby S. 2014. Biolistic transformation of wheat with centrophenoxine as a synthetic auxin. *Methods in molecular biology* **1145**: 191-202.

Ivanova A, Law SR, Narsai R, Duncan O, Lee JH, Zhang B, Van Aken O, Radomiljac JD, van der Merwe M, Yi K, et al. 2014. A Functional Antagonistic Relationship between Auxin and Mitochondrial Retrograde Signaling Regulates Alternative Oxidase1a Expression in Arabidopsis. *Plant Physiology* **165**(3): 1233-1254.

Jia W, Li B, Li S, Liang Y, Wu X, Ma M, Wang J, Gao J, Cai Y, Zhang Y, et al. 2016. Mitogen-Activated Protein Kinase Cascade MKK7-MPK6 Plays Important Roles in Plant Development and Regulates Shoot Branching by Phosphorylating PIN1 in Arabidopsis. *PLoS Biol* **14**(9): e1002550.

Krouk G, Lacombe B, Bielach A, Perrine-Walker F, Malinska K, Mounier E, Hoyerova K, Tillard P, Leon S, Ljung K, et al. 2010. Nitrate-Regulated Auxin Transport by NRT1.1 Defines a Mechanism for Nutrient Sensing in Plants. *Developmental Cell* **18**(6): 927-937.

Kubo M, Imai A, Nishiyama T, Ishikawa M, Sato Y, Kurata T, Hiwatashi Y, Reski R, Hasebe M. 2013. System for stable beta-estradiol-inducible gene expression in the moss Physcomitrella patens. *PLoS One* **8**(9): e77356.

Ludwig-Muller J. 2014. Auxin homeostasis, signaling, and interaction with other growth hormones during the clubroot disease of Brassicaceae. *Plant signaling & behavior* **9**(4): e28593.

Michniewicz M, Zago MK, Abas L, Weijers D, Schweighofer A, Meskiene I, Heisler MG, Ohno C, Zhang J, Huang F, et al. 2007. Antagonistic regulation of PIN phosphorylation by PP2A and PINOID directs auxin flux. *Cell* **130**(6): 1044-1056.

Mravec J, Skupa P, Bailly A, Hoyerova K, Krecek P, Bielach A, Petrasek J, Zhang J, Gaykova V, Stierhof YD, et al. 2009. Subcellular homeostasis of phytohormone auxin is mediated by the ER-localized PIN5 transporter. *Nature* **459**(7250): 1136-1140.

Muller A, Duchting P, Weiler EW. 2002. A multiplex GC-MS/MS technique for the sensitive and quantitative single-run analysis of acidic phytohormones and related compounds, and its application to Arabidopsis thaliana. *Planta* **216**(1): 44-56.

Muller D, Leyser O. 2011. Auxin, cytokinin and the control of shoot branching. *Ann Bot* **107**(7): 1203-1212.

Nagy SK, Meszaros T. 2014. In Vitro Translation-Based Protein Kinase Substrate Identification. *Cell-Free Protein Synthesis: Methods and Protocols* **1118**: 231-243.

Nina Theis, Manuel Lerdau. 2003. The Evolution of Function in Plant Secondary Metabolites. *International Journal of Plant Sciences* **164**(S3): S93-S102.

Nisar N, Cuttriss AJ, Pogson BJ, Cazzonelli CI. 2014. The promoter of the Arabidopsis PIN6 auxin transporter enabled strong expression in the vasculature of roots, leaves, floral stems and reproductive organs. *Plant Signal Behav* **9**(1): e27898.

Okada K, Ueda J, Komaki MK, Bell CJ, Shimura Y. 1991. Requirement of the Auxin Polar Transport System in Early Stages of Arabidopsis Floral Bud Formation. *The Plant Cell Online* **3**(7): 677-684.

804 **Ottenschlager I, Wolff P, Wolverton C, Bhalerao RP, Sandberg G, Ishikawa H, Evans**
805 **M, Palme K. 2003.** Gravity-regulated differential auxin transport from columella to
806 lateral root cap cells. *Proc Natl Acad Sci U S A* **100**(5): 2987-2991.
807 **Paponov IA, Teale WD, Trebar M, Blilou I, Palme K. 2005.** The PIN auxin efflux
808 facilitators: evolutionary and functional perspectives. *Trends in Plant Science* **10**(4):
809 170-177.
810 **Peer WA, Blakeslee JJ, Yang H, Murphy AS. 2011.** Seven Things We Think We Know
811 about Auxin Transport. *Mol Plant* **4**(3): 487-504.
812 **Petersen M, Brodersen P, Naested H, Andreasson E, Lindhart U, Johansen B, Nielsen**
813 **HB, Lacy M, Austin MJ, Parker JE, et al. 2000.** Arabidopsis MAP kinase 4
814 negatively regulates systemic acquired resistance. *Cell* **103**(7): 1111-1120.
815 **Petrasek J, Mravec J, Bouchard R, Blakeslee JJ, Abas M, Seifertova D, Wisniewska J,**
816 **Tadele Z, Kubes M, Covanova M, et al. 2006.** PIN proteins perform a rate-limiting
817 function in cellular auxin efflux. *Science* **312**(5775): 914-918.
818 **Pitzschke A, Schikora A, Hirt H. 2009.** MAPK cascade signalling networks in plant
819 defence. *Curr Opin Plant Biol* **12**(4): 421-426.
820 **Pritchard CC, Cheng HH, Tewari M. 2012.** MicroRNA profiling: approaches and
821 considerations. *Nature reviews. Genetics* **13**(5): 358-369.
822 **Rasmussen A, Hosseini SA, Hajirezaei MR, Druege U, Geelen D. 2015.** Adventitious
823 rooting declines with the vegetative to reproductive switch and involves a changed
824 auxin homeostasis. *Journal of Experimental Botany* **66**(5): 1437-1452.
825 **Riegler J, Ditengou F, Palme K, Nann T. 2008.** Blue shift of CdSe/ZnS nanocrystal-labels
826 upon DNA-hybridization. *J Nanobiotechnology* **6**: 7.
827 **Rodriguez MC, Petersen M, Mundy J. 2010.** Mitogen-activated protein kinase signaling in
828 plants. *Annual Review of Plant Biology, Vol 63* **61**: 621-649.
829 **Sabatini S, Beis D, Wolkenfelt H, Murfett J, Guilfoyle T, Malamy J, Benfey P, Leyser O,**
830 **Bechtold N, Weisbeek P, et al. 1999.** An auxin-dependent distal organizer of pattern
831 and polarity in the Arabidopsis root. *Cell* **99**: 463-472.
832 **Sawchuk MG, Edgar A, Scarpella E. 2013.** Patterning of Leaf Vein Networks by
833 Convergent Auxin Transport Pathways. *PLoS Genetics* **9**(2).
834 **Scarpella E, Francis P, Berleth T. 2004.** Stage-specific markers define early steps of
835 procambium development in Arabidopsis leaves and correlate termination of vein
836 formation with mesophyll differentiation. *Development* **131**(14): 3445-3455.
837 **Shen CJ, Yue RQ, Sun T, Zhang L, Yang YJ, Wang HZ. 2015.** OsARF16, a transcription
838 factor regulating auxin redistribution, is required for iron deficiency response in rice
839 (Oryza sativa L.). *Plant Science* **231**: 148-158.
840 **Simon S, Skůpa P, Viaene T, Zwiewka M, Tejos R, Klíma P, Čarná M, Rolčík J, De**
841 **Rycke R, Moreno I, et al. 2016.** PIN6 auxin transporter at endoplasmic reticulum and
842 plasma membrane mediates auxin homeostasis and organogenesis in Arabidopsis. *New*
843 *Phytol* **211**(1): 65-74.
844 **Suer S, Agusti J, Sanchez P, Schwarz M, Greb T. 2011.** WOX4 Imparts Auxin
845 Responsiveness to Cambium Cells in Arabidopsis. *Plant Cell* **23**(9): 3247-3259.
846 **Sundaresan V, Springer P, Volpe T, Haward S, Jones JD, Dean C, Ma H, Martienssen**
847 **R. 1995.** Patterns of gene action in plant development revealed by enhancer trap and
848 gene trap transposable elements. *Genes Dev* **9**(14): 1797-1810.
849 **Thimann KV. 1939.** Auxins and the inhibition of plant growth. *Biological Reviews* **14**(3):
850 314-337.
851 **Turi CE, Axwik KE, Smith A, Jones AM, Saxena PK, Murch SJ. 2014.** Galanthamine, an
852 anti-cholinesterase drug, effects plant growth and development in Artemisia tridentata
853 Nutt. via modulation of auxin and neurotransmitter signaling. *Plant signaling &*
854 *behavior* **9**(4): e28645.

Ugartechea-Chirino Y, Swarup R, Swarup K, Peret B, Whitworth M, Bennett M, Bougourd S. 2010. The AUX1 LAX family of auxin influx carriers is required for the establishment of embryonic root cell organization in Arabidopsis thaliana. *Annals of Botany (London)* **105**(2): 277-289.

Weiste C, Droge-Laser W. 2014. The Arabidopsis transcription factor bZIP11 activates auxin-mediated transcription by recruiting the histone acetylation machinery. *Nature Communications* **5**: 3883.

Wilson M, Goh T, Voss U, Bishopp A, Peret B, Bennett M. 2013. SnapShot: Root development. *Cell* **155**(5): 1190-1190 e1191.

Wolters H, Jurgens G. 2009. Survival of the flexible: hormonal growth control and adaptation in plant development. *Nature Reviews Genetics* **10**(5): 305-317.

Xu J, Zhang SQ. 2015. Mitogen-activated protein kinase cascades in signaling plant growth and development. *Trends in Plant Science* **20**(1): 56-64.

Zhang S, D ZH, Yang C. 2014. AtFtsH4 perturbs the mitochondrial respiratory chain complexes and auxin homeostasis in Arabidopsis. *Plant signaling & behavior* **9**(9): e29709.

Zourelidou M, Absmanner B, Weller B, Barbosa IC, Willige BC, Fastner A, Streit V, Port SA, Colcombet J, de la Fuente van Bentem S, et al. 2014. Auxin efflux by PIN-FORMED proteins is activated by two different protein kinases, D6 PROTEIN KINASE and PINOID. *eLife* **3**.

Zulawski M, Schulze G, Braginets R, Hartmann S, Schulze WX. 2014. The Arabidopsis Kinome: phylogeny and evolutionary insights into functional diversification. *BMC Genomics* **15**: 548.

Supporting information

Fig. S1 *PIN6* expression during plant development

Fig. S2 Specificity of anti-PIN6 antibody

Fig. S3 Localization of PIN6 and auxin distribution at the root tip

Fig. S4 Evolutionarily conserved PINOID phosphorylation sites in AtPIN6 and PIN6-like proteins

Fig. S5 A basal-to-apical shift in PM-resident PIN6 localization in plants overexpressing PINOID kinase

Fig. S6 Phosphorylated residues in PIN proteins

Fig. S7 ER-localized PIN6 is insensitive to BFA

Fig. S8 The PIN6 phosphorylation sites T392 and T393 are involved in plant growth and plant inflorescence stem elongation

Fig. S9 Inflorescence stem development

892 **Fig. S10** Developmental control of PIN6 subcellular localization

893 **Table S1 List of primers used**

894 **Methods S1** Characterization of *pin6* mutants and generation of transgenic lines

895 **Methods S2** Free IAA level determination

896 **Methods S3** Immunolocalization

897 **Methods S4** Quantitative RNA analysis

898 **Methods S5** Microscopy and image post processing

899

900 **Notes S1** Methods references

901 **Video/Movie S1** Z-stack maximum projection of confocal microscope images showing

902 PM-located PIN6$^{T392E/T393E}$

903 **Video/Movie S2** Z-stack maximum projection of confocal microscope images showing

904 ER-located PIN6$^{T392V/T393V}$

905

906

907

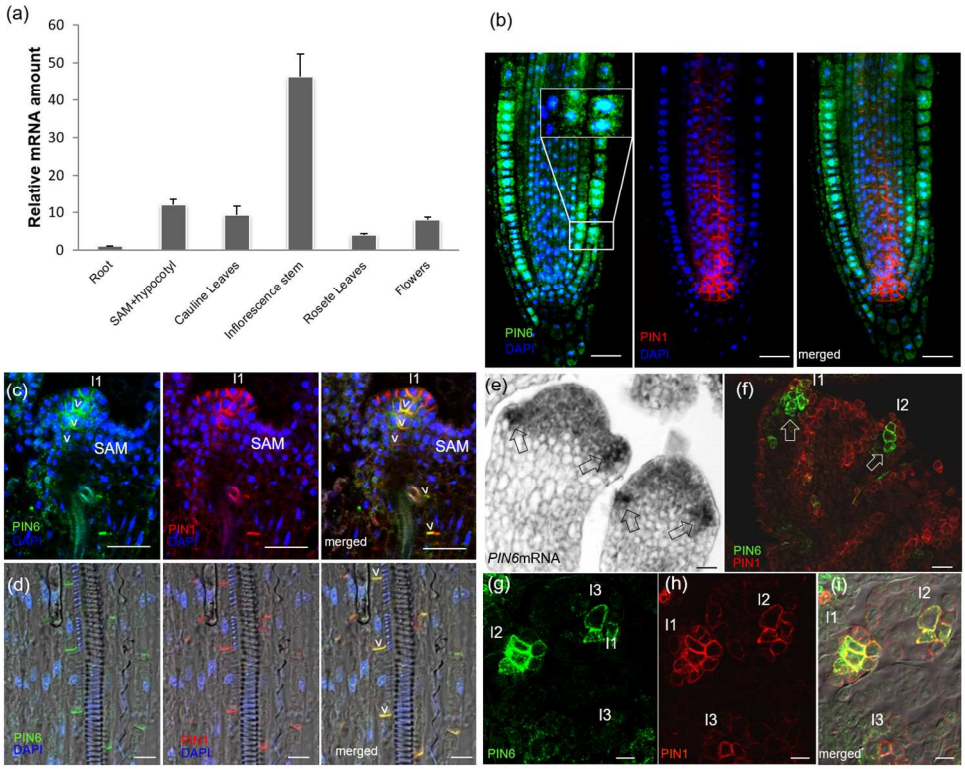

Figure 1. PIN6 expression and subcellular localization.
(a) PIN6 mRNA levels in different tissues were detected by qRT-PCR. (b-c) Immunolocalization of PIN6 and PIN1 in Arabidopsis WT seedlings. (b) Immunocytolocalization of PIN6 and PIN1 in a seedling root tip. PIN6 is mainly cytoplasmic in endomembrane domains. (c) PIN6 is localized mainly at the PM of developing vegetative leaf primordium and co-localizes with PIN1. (d), Co-localization of PIN6 and PIN1 at the PM in stem xylem parenchyma cells. (e) PIN6 expression in developing WT flowers. Arrows indicate PIN6 mRNA. (f-g), Immunolocalization of PIN6 and PIN1 in Arabidopsis inflorescences. (f) PIN6 and PIN1 subcellular localization in an inflorescence longitudinal section. Arrow indicates PIN6 localization at the PM in emerging incipient primordia (I1, I2). (g-i) Co-localization of PIN6 and PIN1 at the PM in WT Arabidopsis inflorescence transverse sections. (g), PM-localized PIN6 (green). (h) PM-localized PIN1 (red). (I) G and H merged. PIN6 and PIN1 co-localize at the PM in incipient leaf primordia (I1, I2, I3) tips. Scale bars, 20 μM in (b), (c), (e), (f), (g), (h), and (i); 10 μm in (d).

124x98mm (300 x 300 DPI)

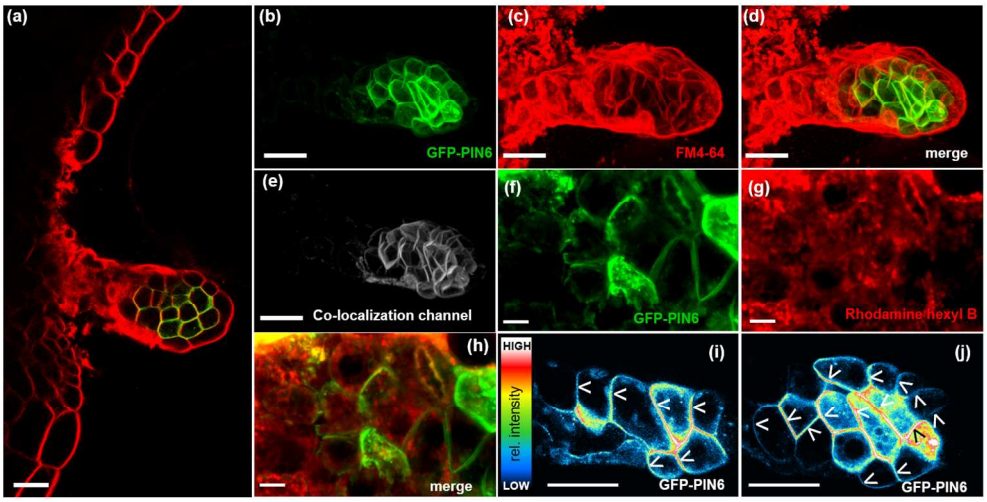

Figure 2. PIN6 is located at the PM in WT Arabidopsis nectary glands.
(a) WT plants expressing a pPIN6::GFP-PIN6 fusion protein in nectary glands were labelled with endosome tracker/PM marker FM4-64. (b-e) Z-stack maximum projection of confocal microscope images showing GFP-PIN6 co-localizing with FM4-64. (b) GFP-PIN6 signal. (c), FM4-64 signal. (d), (b) and (c) merged. (e), Co-localization of GFP-PIN6 and FM4-64 in (D). (f-h) WT plants expressing a pPIN6::GFP-PIN6 fusion in nectary glands labelled with the ER marker rhodamine B hexyl ester. GFP-PIN6 is not localized to the ER. (f) GFP-PIN6 signal. (g) Rhodamine hexyl B signal. (h) (f) and (g) merged. (i-j) Semi-quantitative, color-coded heat map of PM-PIN6 displaying GFP-PIN6 polarity in confocal microscope virtual sections of a WT nectary. Dark and white pixels indicate low and high intensity, respectively; pixel values range from 0 to 4095. (i) Outer plane of the nectary gland. (j) Median plane of the nectary. Arrowheads indicate GFP-PIN6 polarity. Scale bar, 20 µm.

567x290mm (72 x 72 DPI)

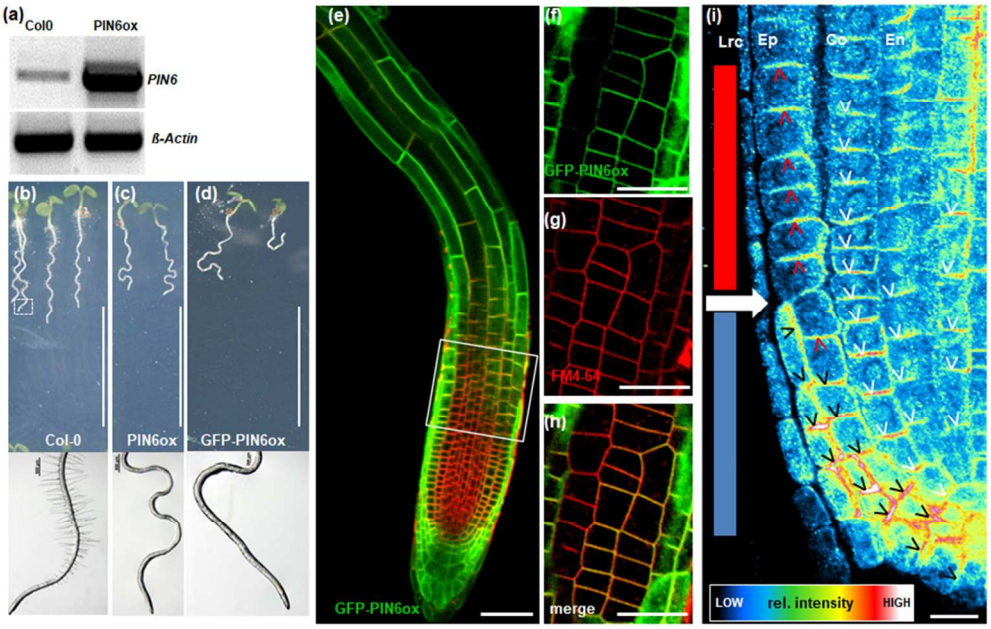

Figure 3. PM targeting of PIN6 in PIN6ox plants.
(a) PIN6 and ß-Actin (as a reference gene) mRNA levels were detected by RT-PCR in WT (Col-0) and 35S::PIN6 (PIN6ox) Arabidopsis seedlings. (b-d) PIN6 overexpression perturbs root growth (upper panel) and abolishes root hair development (lower panel). (b) Col-0. (c) 35S::PIN6 (PIN6ox). (d) 35S::GFP-PIN6 (GFP-PIN6ox). (e) Overexpressed GFP-PIN6 (GFP-PIN6ox) co-localizes with the PM marker FM4-64. (f-h) Magnified view of epidermal cells showing co-localization of GFP-PIN6ox and FM4-64 at the PM. (i) Color-coded heat map showing high and low AtPIN6 signal intensities detected with the anti-PIN6 antibody. The solid white arrow marks the separation between meristematic cells of the epidermis in Tier 1 (red box) and Tier 2 (blue box). In Tier 1, PIN6 localizes apically (toward the shoot; red arrowheads), while in Tier 2, PIN6 localizes basally (toward the quiescent centre; black arrowheads). White arrowheads indicate PIN6 polarity in the cortex, endodermis and stele cells. Epidermis (Ep), cortex (Co), endodermis (En), lateral root cap cells (Lrc). Scale bar, 1 cm in a-c, 50 µm in e, and 20 µm in f-h and i.

75x47mm (300 x 300 DPI)

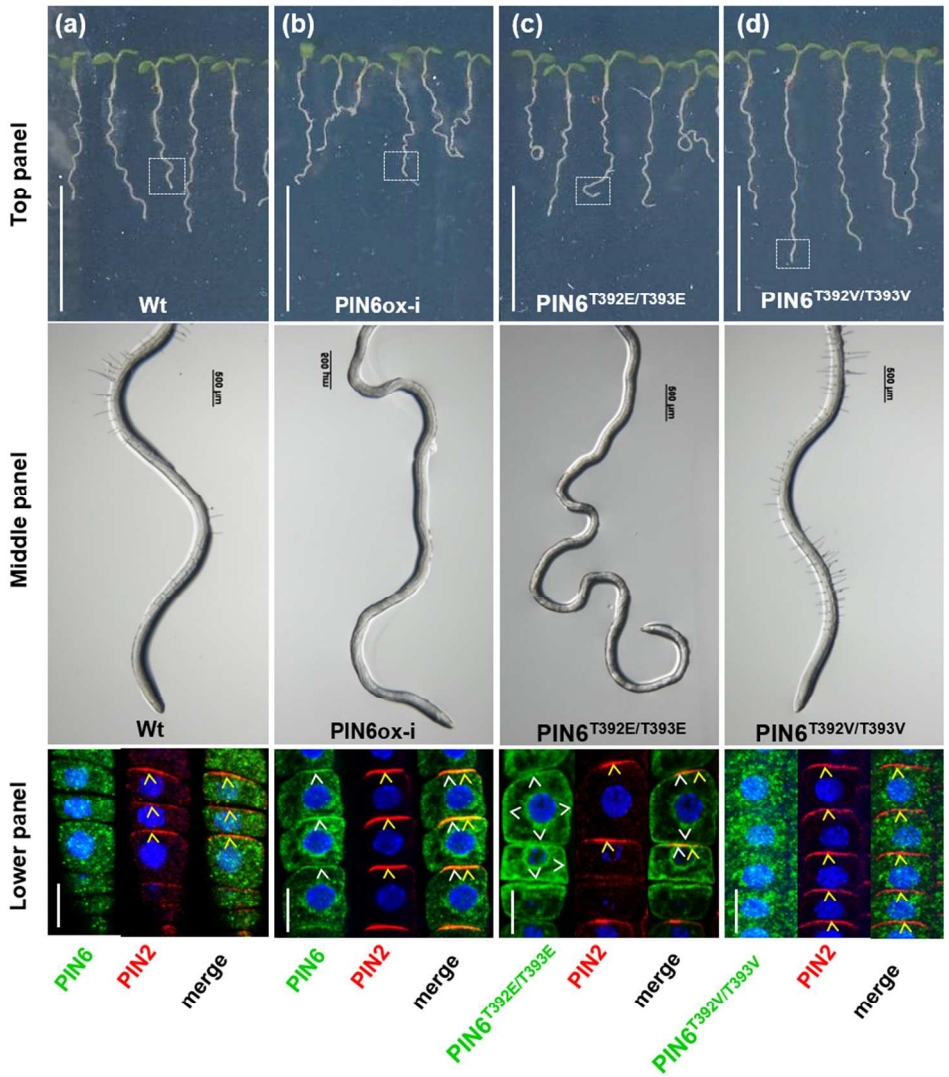

Figure 4. PIN6 ER exit is phosphorylation dependent. Four-day-old wild-type (WT) Arabidopsis and PIN6-inducible lines were induced with 0.1 μM β-estradiol for 3 days. (a) Neither the growth (top panel) nor root hair development (middle panel) of WT plants is affected. In the root tip epidermal cells (lower panel), immunolocalization shows that PIN6 localizes in endomembrane compartments, while PIN2 is detected at the PM. (b) After induction with β-estradiol, PIN6ox-i root growth is affected (top panel), root hair development is suppressed (middle panel) and PIN6 is targeted to the PM, where it colocalizes with PIN2 (lower panel). (c) Induced roots of EE plants are agravitropic (top panel) and hairless (middle panel), with GFP-PIN6 (detected with an anti-GFP antibody) being predominantly localized apolarly at the PM, where it partially co-localizes with PIN2 (lower panel). (d), Induced VV plants are not affected by β-estradiol induction (top and middle panels). GFP-PIN6 is predominantly localized in the ER. White and yellow arrowheads indicate PM-PIN6 and PM-PIN2, respectively, and nuclei are stained in blue with DAPI. Scale, 1 cm (top panel) and 10 μM (lower panel).

90x100mm (300 x 300 DPI)

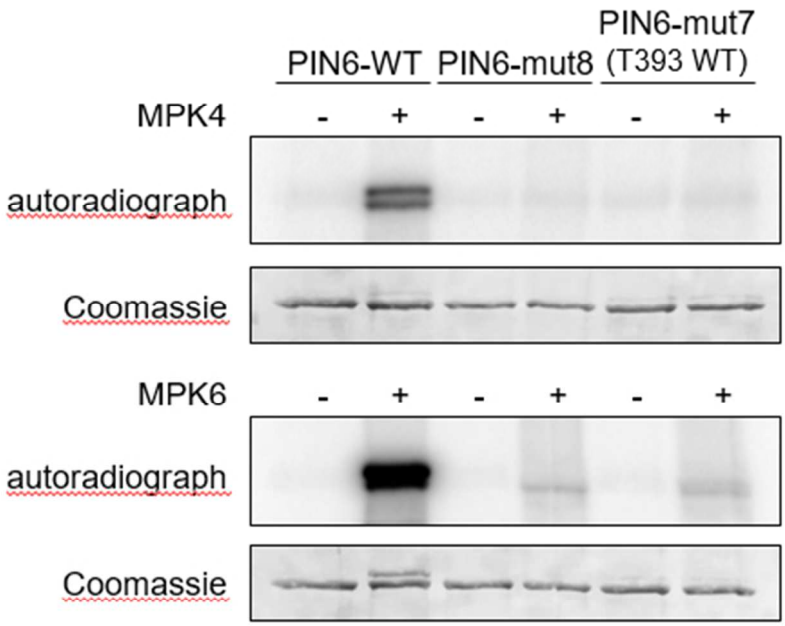

Figure 5. PIN6 is phosphorylated by MPK4 and MPK6. Kinase assay with in vitro-translated, affinity-purified WT GST:PIN6 (PIN6-WT), T226A, T242A, S286A, T304A, T320A, S326A, S337A, and T393A mutant GST:PIN6 (indicated as 'PIN6-mut8') and T226A, T242A, S286A, T304A, T320A, S326A and S337A mutant [indicated as 'PIN6-mut7 (T393-WT)'] GST:PIN6 variants. PIN6 variants were incubated in the absence (-) or presence (+) of in vitro-translated, affinity-purified, activated MPK4 (top panel) or MPK6 (bottom panel). Protein loading is visualized by Coomassie staining.

46x36mm (300 x 300 DPI)

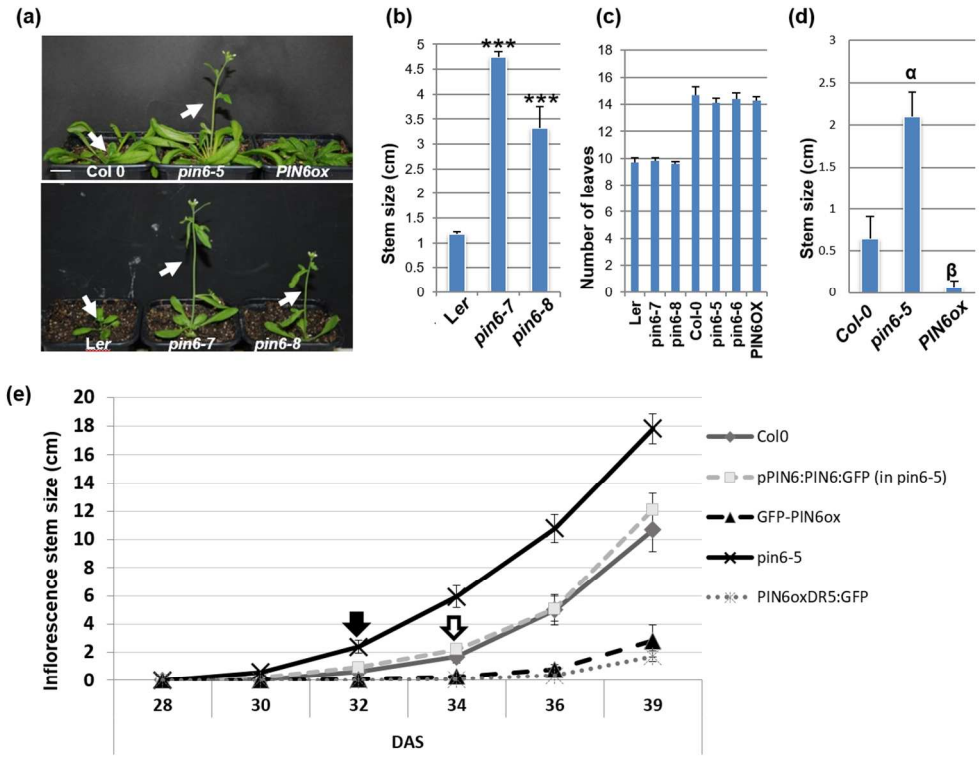

Figure 6. PIN6 regulates Arabidopsis inflorescence stem elongation.
(a) WT Col-0, pin6-5, PIN6ox, WT Ler, pin6-7 and pin6-8 plants were grown in soil for 35 days (Col-0, pin6-5 and PIN6ox) or 23 days (Ler, pin6-7 and pin6-8). Scale bar, 1 cm. (b) pin6-6 and pin6-7 inflorescence stems are significantly longer than WT Ler inflorescence stems. Stars (*) indicate significant differences from WT control at P<0.01 (T-test). The data are shown as means (n=40 ± s.e.). (c) At flowering, pin6 mutants and WT plants display the same number of rosette leaves. (d) The inflorescence stem is significantly longer in pin6-5 plants than WT Col-0 plants, while PIN6ox plant inflorescence stems are significantly shorter. (e) Quantification of the inflorescence stem development of WT Col-0, pin6-5 mutant, pin6-5 complemented with pPIN6::PIN6-GFP, GFP-PIN6ox and PIN6oxDR5::GFP plants. DAS, days after sowing seeds. Symbols (α, β) in (d) indicate significant differences, as determined by ANOVA followed by Tukey's Honest significant difference (HSD) post hoc test (P<0.05). The data are shown as means (n=20 ± s.e.).

111x86mm (300 x 300 DPI)

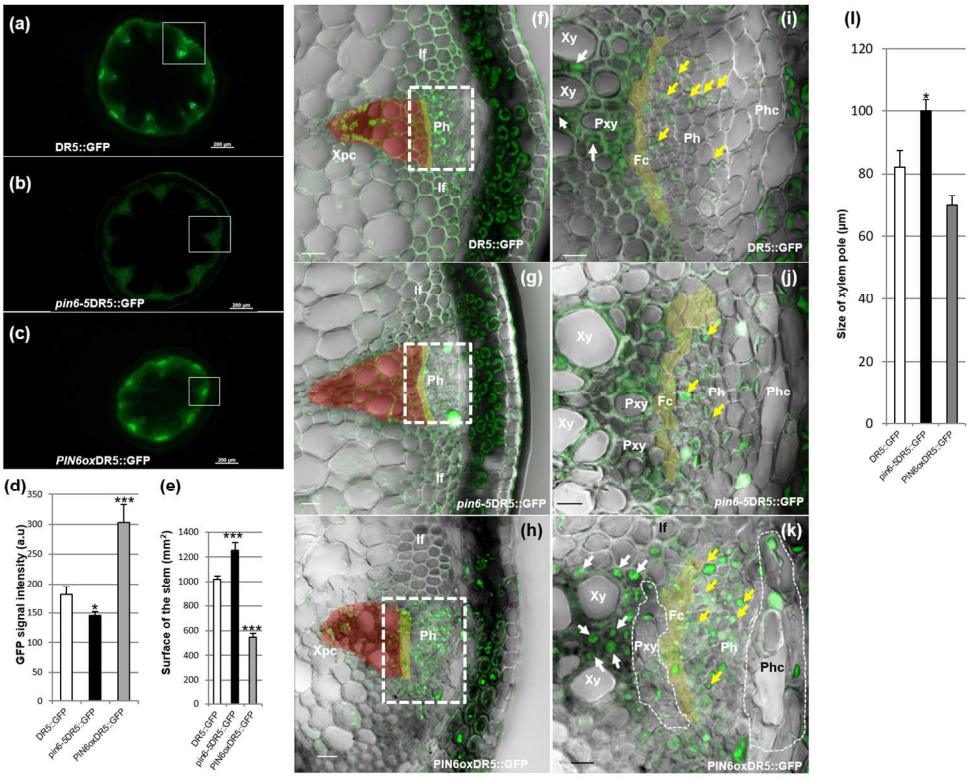

Figure 7. Auxin distribution and vascular tissue differentiation. Transverse sections taken 50 mm above the uppermost rosette leaf of the inflorescence stem of DR5rev::GFP, pin6-5DR5rev::GFP and PIN6oxDR5rev::GFP plants. (a), GFP signal in DR5rev::GFP vascular bundles. (b) GFP signal in pin6-5DR5rev::GFP vascular bundles. Note the reduction in DR5rev::GFP signal. (c) GFP signal in PIN6oxDR5rev::GFP vascular bundles. Note the increase in DR5rev::GFP signal. (d) Quantification of GFP signal from plants shown in (a), (b), and (c). (e) Stem surface area of plants shown in (a), (b), and (c). (f) Boxed area in (a). (g) Boxed area in (b). (h) Boxed area in (c). (i) Magnified view of boxed area in (f). Note the GFP signal in phloem cells (Ph, yellow arrows) and xylem parenchyma cells (Xpc, white arrows). (j) Magnified view of boxed area in (g). Note the reduced number of Xpc.
(k) Magnified view of boxed area in (h). Note the DR5rev::GFP signal in nearly all phloem cells (yellow arrows), the increased number of Xpc displaying DR5rev::GFP signal (white arrows) and the presence of protoxylem cells (Pxy) and phloem cap cells (Phc) with an abnormal shape (dashed circles). Xylem tissues (Xy) and fascicular cambium cells (Fc) are overlaid in red and yellow, respectively. Interfascicular cambium (If). (l), Size of xylem pole. Stars (*) or (***) indicate significant differences at $P<0.05$ or $P<0.01$ (T-test), respectively. The data are shown as means (n=11-17 ± s.e. for (d); n=8 ± s.e. for (e); n=16-22 for (m). Scale bar, 20 µm in (f-h), 10 µm in (i-k).

133x103mm (300 x 300 DPI)